

https://dspace.org/

Suspect screening of perand polyfluoroalkyl substances in paper by selective and nonselective extraction with UHPLCQ orbitrap MS

Nondumiso Mofokeng; L Madikizela; I Tiggelman; E Sanganyado; Luke Chimuka

PERGAMON-ELSEVIER SCIENCE LTD
https://hdl.handle.net/10539/42217
WOS

Downloaded from a DSpace repository. https://dspace.org/

Chemosphere 363 (2024) 142904

Contents lists available at ScienceDirect

Chemosphere

journal homepage: www.elsevier.com/locate/chemosphere

Suspect screening of per-and polyfluoroalkyl substances in paper by selective and non-selective extraction with UHPLC-Q orbitrap MS

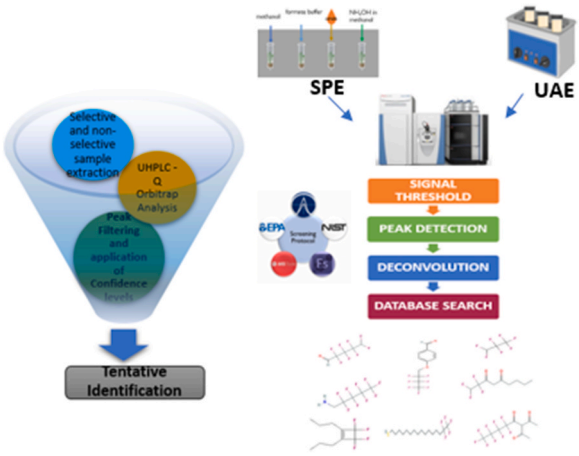
Nondumiso N. Mofokeng [a,b,*], Lawrence M. Madikizela [c], Ineke Tiggelman [b], Edmond Sanganyado [d], Luke Chimuka [a]

[a] Molecular Sciences Institute, School of Chemistry, University of the Witwatersrand, 1 Jan Smuts Ave, Braamfontein, Johannesburg, 2000, South Africa
[b] Mpact Innovation, Research & Development, Devon Valley Road, Stellenbosch, 7600, South Africa
[c] Institute for Nanotechnology and Water Sustainability, College of Science, Engineering and Technology, University of South Africa, Florida Science Campus, 28 Pioneer Ave, Roodepoort, Johannesburg, 1709, South Africa
[d] Department of Applied Sciences, Northumbria University, Newcastle upon Tyne, NE1 8ST, United Kingdom

HIGHLIGHTS

- Two extraction techniques were employed for PFAS suspect screening of paper.
- ASE with WAX SPE for selective extraction and UAE for non-selective extraction.
- 41 unique PFAS tentatively identified with 3 common to both pre-treatment techniques.
- Per- and polyfluoroalkyl ketones, diketones and amines were predominantly identified.
- Study showed the influence of method selectivity in the detected PFAS.

GRAPHICAL ABSTRACT



ARTICLE INFO

Handling editor: Myrto Petreas

Keywords:
Untargeted analysis
High resolution mass spectrometry
Solid phase extraction
Ultrasonic
Chromatography
Recycled paper

ABSTRACT

Non-targeted analysis and suspect screening of per- and polyfluoroalkyl substances (PFAS) in various matrices have gained traction with advancements in accurate mass analytical instruments. This study employed ultra-high performance liquid chromatography coupled to quadrupole orbitrap high-resolution mass spectrometry for PFAS suspect screening of paper grades used in the paper recycling chain. The samples were prepared using two extraction techniques; selective accelerated solvent extraction with weak anionic exchange solid-phase extraction and non-selective ultrasonic-assisted extraction. A suspect screening protocol was established to tentatively identify suspected PFAS against spectral databases using a systematic approach of peak filtering and study-specific thresholds for reporting, linked to a confidence level. The possible prevalence of previously

* Corresponding author. Molecular Sciences Institute, School of Chemistry, University of the Witwatersrand, 1 Jan Smuts Ave, Braamfontein, Johannesburg, 2000, South Africa.
E-mail address: nmofokeng@mpact.co.za (N.N. Mofokeng).

https://doi.org/10.1016/j.chemosphere.2024.142904
Received 5 June 2024; Received in revised form 17 July 2024; Accepted 17 July 2024
Available online 19 July 2024
0045-6535/© 2024 The Authors. Published by Elsevier Ltd. This is an open access article under the CC BY-NC-ND license (http://creativecommons.org/licenses/by-nc-nd/4.0/).

unreported PFAS in several paper materials across the various collection sites in the paper recycling chain was inferred by the common detection of short-chain polyfluoroalkyl ketones and diketones in the paper recycling chain. The suspect screening tentatively identified 41 unique PFAS, with 3 common to both pre-treatment techniques. The detection of unique PFAS by the two sample pre-treatment techniques highlighted the significance of both selective and non-selective extraction in PFAS screening endeavours. Further, it showed the importance of understanding the acquisition mechanisms employed in mass spectrometry where data-dependent acquisition triggered fragmentation in certain identified compounds, and not in others. The tentatively identified PFAS indicated that there were several previously unreported PFAS in the paper recycling chain and that additional studies were required to investigate their abundance, possible persistence, bioaccumulation and toxicity, in relation to their functional groups and carbon chains.

1. Introduction

The analysis of per- and polyfluoroalkyl substances (PFAS) in various samples has become synonymous with the detection of perfluoroalkyl carboxylic acids and sulfonic acids (Al Amin et al., 2020). However, PFAS include a wide range of chemical classes and functional groups, including esters, betaines, hydrofluoroethers, chlorofluoro olefins, fluoropolymers, fluorotelomers, aromatics, amines, ethers, and benzamides (Berhanu et al., 2023; Bugsel et al., 2023). The need for further exploration of a wider range of compounds has led to an increasing need for screening and non-targeted approaches (Houtz et al., 2018; Liu et al., 2019, 2022; Wang et al., 2022; Bugsel et al., 2023; Zweigle et al., 2023). Such an exploration is often hindered by several challenges associated with PFAS analysis. The first challenge is the large number of compounds in this class. PFAS consist of over 10 000 compounds (Tang et al., 2023), when defined as any fluorinated compound with at least one fully fluorinated methyl group and including a broad range of compounds from small molecules to complex aromatics and polymers (Wang et al., 2021). These are manufactured for numerous applications (Glüge et al., 2020) using various undisclosed and unreported synthesis pathways that result in intermediates, precursors, and degradation products (Shen et al., 2023). The number of PFAS that have been identified thus far pales in comparison to the number of analytical standards available (Bugsel et al., 2023; Manojkumar et al., 2023). Ubiquitous PFAS contamination and instrument capabilities (Manojkumar et al., 2023) are other challenges associated with untargeted PFAS detection. High-resolution mass spectrometry (HRMS) is a powerful tool for addressing some of these challenges to identify known, novel, and/or emerging PFAS (Manojkumar et al., 2023; Stroski and Sapozhnikova, 2023). In the absence of reference standards, confidence intervals have been used to assess the tentatively identified compounds (Charbonnet et al., 2022). Charbonnet et al. (2022) proposed a confidence scheme for screening and non-target analysis of PFAS from Levels 1 to 5, where Level 1 indicates the greatest confidence (by reference standard and MS^2) and Level 5 the least confident identification (validated by comparison with exact mass (Charbonnet et al., 2022). In the case of suspected screening, matching the expected exact mass, isotope pattern formation, and product ions strengthens the probability of correct identification (Hajeb et al., 2022).

For liquid chromatography in tandem with mass spectrometry, the quality of the results obtained in PFAS screening often lies in the extraction and ionization efficiency. Complex materials, such as paperboard, consist of a complex matrix of chemicals used in manufacturing and conversion processes. These chemicals include organic and inorganic compounds, salts, and polymeric compounds. These compounds influence the resultant sample matrix constituents and can significantly affect the detection of PFAS (Dickman and Aga, 2022). Matrix effects influence the ionization efficiency and signal response (Shen et al., 2023). To reduce these effects, pre-treatment or purification procedures are employed to influence both the selectivity and sensitivity of the analyses (Hajeb et al., 2022). For suspect screening, the sample pre-treatment steps should ideally extract a wide range of PFAS compounds while minimizing interfering matrix elements that may adversely impact identification. HRMS has been found to significantly reduce interference from matrices, allowing for a degree of flexibility in enhancing the sensitivity of ultra-trace PFAS analysis (Al Amin et al., 2020). Supported liquid extraction (SLE), pressurized liquid extraction (PLE) (also referred to accelerated solvent extraction (ASE)), ultrasonic-assisted extraction (UAE), and solid phase extraction (SPE) are common extraction techniques for PFAS detection in solid matrices, such as soil, sediment, food packaging, and sludge (Al Amin et al., 2020; Hajeb et al.,. 2022). Suspected PFAS screening has been undertaken on various food packaging matrices (Hajeb et al., 2022; Boisacq et al., 2023; Sapozhnikova et al., 2023); however, reports on non-food packaging are limited. The circularity of paper recycling means that unknown PFAS may propagate among recycled paper manufacturing, paper recycling, waste mingling, consumers, and the environment. Therefore, it is important to explore the nature of PFAS that may be present and generate new knowledge in the research area.

In this study, suspected screening of recycling paper grades was investigated using two sample pre-treatment techniques; ASE with SPE and UAE in order to compare the detection and chemical properties of the resulting tentatively identified PFAS. Various grades of paper were sourced from paper mills and conversion sites (pre-consumer), grocery store (i.e., supermarket store with both food and non-food packaging) (retail), domestic waste sites, solid waste disposal sites, waste pickers, and recycling facilities (post-consumer) in Cape Town, South Africa. Analysis was performed using ultra-high-performance liquid chromatography – high-resolution mass spectrometry (UHPLC-HRMS) Orbitrap.

2. Materials and methods

2.1. Chemicals and sampling

LC-MS-grade methanol, ethanol, and water, as well as HPLC-grade formic acid, toluene, ammonium formate, and analytical grade ammonium hydroxide solution were purchased from Merck (Johannesburg, South Africa) and Anatech (Cape Town, South Africa). These chemicals and buffers were used as received without further purification (Table S1). Thirty-nine paper samples were collected from Cape Town, South Africa, consisting of various grades of paper used for recycling. The pre-consumer and retail samples consisted only of paperboard, whereas the post-consumer samples consisted of paper grades typically used in the manufacture of recycled boards. These included cartons, newspapers, corrugated boxes, office paper, and magazines. Pre-consumer samples were sourced directly from paper mills and paper conversion sites, whereas retail samples were collected from South African grocery stores. Post-consumer samples were collected from recycling facilities, solid waste disposal sites, household waste, and informal waste pickers. The collected samples were placed in polypropylene (PP) sleeves and polyethylene (PE) bags prior to sample pre-treatment.

2.2. Sample pre-treatment

The samples were first shredded using a kitchen blender to a dry pulp consistency for the two pre-treatment techniques: ASE with SPE and UAE. Paper samples were prepared in triplicate (0.5 g each) using an analytical balance (Table S2) and extracted using a Dionex 350 ASE

system (Anatech, Cape Town, South Africa). The extraction conditions consisted of a 3:2 ethanol: methanol solvent combination at 70 °C oven temperature for three cycles of 12 min each. After extraction, the sample was evaporated to approximately 1 mL under nitrogen at 40 °C using a Biotage TurboVap (Anatech, Cape Town, South Africa) in preparation for SPE clean-up. Selectivity and specificity were expected to be enhanced based on pH-controlled weak anionic exchange. The selective sample pre-treatment was developed for perfluorocarboxylic acids (PFCAs), perfluorosulfonic acids (PFSAs), and telomeric sulfonates. Enviro-Clean WAX SPE cartridges with a 500 mg sorbent bed (Stargate Scientific, Johannesburg, South Africa) were mounted on an SPE manifold (Stargate Scientific, Johannesburg, South Africa) and operated under vacuum using a DryVac 400 vacuum pump (Air & Vacuum Technologies, Johannesburg, South Africa). The SPE was initiated by conditioning the cartridges with 3 mL of methanol followed by 5 mL of 0.1 M ammonium formate buffer. The supernatant was then loaded (500 μL) before elution with 6 mL of 1% methanolic ammonium hydroxide. The eluent was concentrated to approximately 1 mL under nitrogen at 40 °C using the Biotage TurboVap and filtered into a vial with a 0.22 μm regenerated cellulose syringe filter (Stargate Scientific, Johannesburg, South Africa) filter before analysis by UHPLC-HRMS. The UAE technique aims for less selectivity for a broader class of compounds present in paper-based materials that are generally soluble in polar environments. For sample pre-treatment, 1 g of shredded paper was placed in a 20 mL of 2:1:1 water: ethanol: methanol solution inside a 60 mL glass vial and vortexed for 2 min prior to indirect UAE at 60 °C for 2 h in a sonic bath (Power Sonic 405, United Scientific, Cape Town). The resulting extract was filtered through a 0.22 μm regenerated cellulose syringe filter before analysis by UHPLC-HRMS. Blanks were prepared for both extraction techniques to eliminate any latent PFAS from the suspect screening.

2.3. UHPLC-HRMS parameters

The UHPLC-HRMS was achieved using a Thermo Scientific Vanquish UHPLC$^+$ Q Exactive Focus Orbitrap (Anatech, Cape Town, South Africa) equipped with a Hypersil Gold aQ 100 mm × 2.1 mm x 1.9 μm column and Hypersil Gold 50 mm × 3 mm x 1.9 μm delay column (Anatech, Cape Town, South Africa). Instrument data acquisition was performed using Thermo Scientific Xcalibur and TraceFinder. For the ASE pre-treatment, a binary solvent system was used which consisted of solvent A as 0.1% formic acid in water and 10 mM ammonium formate and methanol as solvent B. The initial flow rate was 0.4 mL min^{-1} in 30% solvent B, which increased to 100% solvent B at 13 min (at 1 mL min^{-1}), held for 17 min, before returning to 30% solvent B at 21.1 min (0.5 mL min^{-1}) (Table S3). The acquisition mode was a full scan with data-dependent acquisition (DDA or ddMS^2) in negative mode. The sample injection volume was 5 μL. The full scan acquisition range was set at 150–750 *m/z* at a resolution of 70 000 with DDA at a resolution of 35 000 (Stroski and Sapozhnikova, 2023). The stepped collision energies were selected as 15 and 30 eV. For the UAE-extracted samples, solvent A consisted of water in 0.1% formic acid with 5 mM ammonium formate, and solvent B as methanol in 0.1% formic acid with 5 mM ammonium formate. The gradient method was initiated at 30% solvent B at 0.3 mL min^{-1} (hold 1 min) before increasing to 100% B, with a curve set at 2 until 15 min. The flow rate was increased to 0.35 mL min^{-1} for 4 min before returning to 30% solvent B and 0.3 mL min^{-1} (Table S3). A 10 μL injection volume was used. The acquisition mode was a full-scan DDA in the negative mode. The full scan acquisition range was 83.4–1250 *m/z* at a resolution of 70 000 and DDA at a resolution of 35 000. The stepped collision energy was selected as 15 and 30 eV.

2.4. Suspect screening methodology

Data analysis was performed using Thermo Scientific Xcalibur TraceFinder 5.0. and FreeStyle 1.8. Two PFAS databases were used for suspect screening: the National Institute of Standards and Technology (NIST) PFAS Suspect List (Place, 2021) and the U.S Environmental Protection Agency (EPA) PFAS Chemicals database (EPA PFAS Chemicals list, 2022) containing 4969 and 10988 PFAS compounds, respectively. Both databases include unique entries that would otherwise be neglected (Bugsel et al., 2023) and allow for increased matching opportunities. The limitation of the NIST suspect list is that it is not a validated list (Place, 2021). An *Unknown screening* data-processing method was developed using TraceFinder. Freestyle was used for mass defect and isotopic pattern verification. Five main factors were used for tentative identification: library database match percentage, accurate mass of the molecular ion, mass tolerance, isotopic pattern match, and MS^2 fragmentation. The accurate mass, mass tolerance, and isotopic pattern match were based on the full-scan acquisition of the molecular ion, taking charge and adduct into consideration. Mass tolerance was defined using Equation (1).

$$\textit{Mass tolerance}\ (ppm) = \left| \frac{\textit{Theoretical mass expected} - \textit{Mass Observed}\ (m/z)}{\textit{Theoretical mass expected}\ (m/z)} \right| \times 10^6 \quad (1)$$

A mass tolerance criterion of ≤10 ppm indicated an accurate mass for suspect screening. The isotopic pattern match was based on a comparison of the theoretical isotopic distribution with the acquired spectrum (Bugsel et al., 2023). This instrument-generated tool was imported to assess the confidence of molecular formula identification by HRMS (Charbonnet et al., 2022). In this study, an acceptable isotopic pattern score was ≥80%, with the number of isotopes matched being ≥ n-1, where n represents all theoretically possible fragments. The MS^2 fragments obtained were used to further enhance the confidence interval for qualitative identification. A confirmatory MS^2 ion was identified for assenting purposes using Thermo Scientific FreeStyle and MStools. Charbonnet et al. (2022) proposed categories for confidence in identifying PFAS using HRMS, where most confidence was categorized as level 1 for most confident matching using a reference standard to least confident identification at level 5, where accurate mass was the only required match criterion. This study aimed for Level 3 identification confidence that considered accurate mass, mass defect, consistent retention time, and isotopic pattern matching with at least one MS^2 fragment linked to a subclass (Charbonnet et al., 2022). The use of mass defects as a PFAS criterion has been extensively used in non-target PFAS analyses (Trier et al., 2011; Baduel et al., 2017; Wang et al., 2018; Liu et al., 2019). However, this filtering process results in false positives for compounds containing other heteroatoms such as sulfur, chlorine, and oxygen (Liu et al., 2019). Getzinger et al. (2021) found that mass defect filtering, although beneficial for filtering out non-PFAS compounds, could also eliminate a large number of potential PFAS. This study showed that PFAS containing nitrogen resulted in higher positive mass defect values than typical PFAS compounds. In this study, the mass defect was therefore used for verification and was not a strict requirement. The mass defect was determined using Thermo Scientific

Freestyle, which subtracted the nominal mass from the exact molecular mass (Getzinger et al., 2021).

2.5. Quality assurance

Preparation blanks of both extraction workflows were prepared to account for any possible PFAS that may have been present in the analytical equipment, solvents and general laboratory consumables. The delay column was fitted between the solvent mixer and autosampler to trap any possible system PFAS. In addition, solvent blanks were inserted between each triplicated sample run to minimise any carry-over. To minimise cross-contamination, prior to each sample the blender was meticulously washed with warm water and detergent, then thoroughly rinsed with deionised water followed by an ethanol rinse before air drying. The stainless steel ASE cells were washed in warm water, rinsed with 1:1 methanol: ethanol, and then placed in an oven for 4 h at 160 °C. The 60 mL borosilicate vials were single-use and discarded after each use. After each use, the vacuum manifold, worktop and laboratory ware used were cleaned with toluene, 1% methanolic ammonium hydroxide followed by methanol.

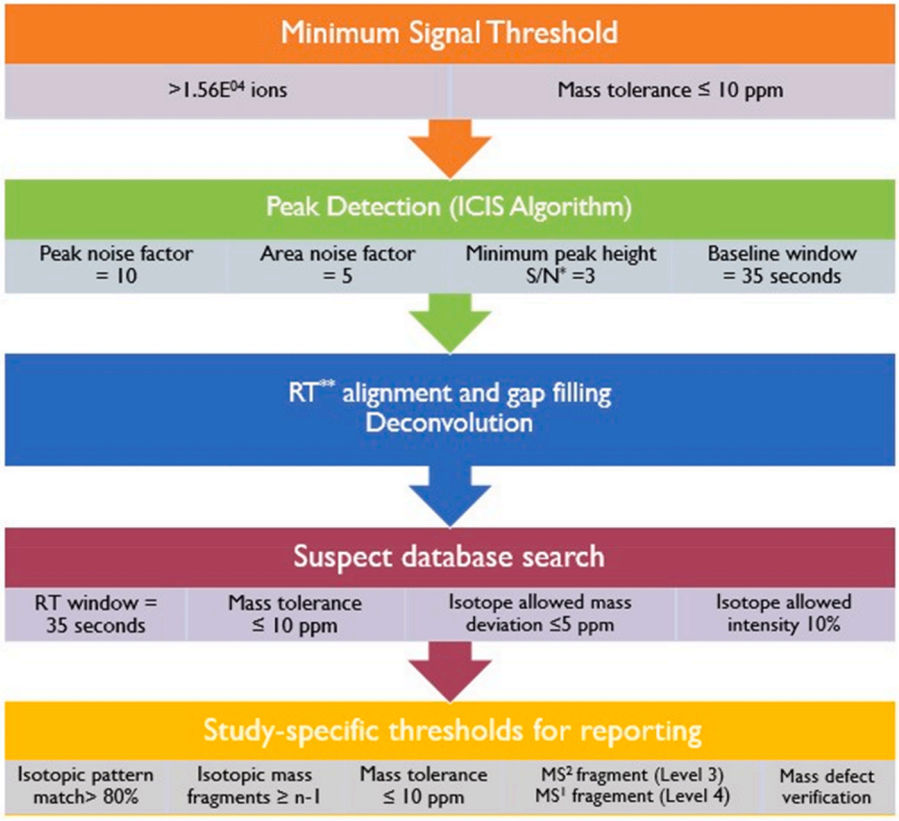
3. Results and discussion

3.1. Suspect PFAS identification workflow

The suspect screening protocol developed in this study is shown in Fig. 1. An unknown analysis data processing method was developed using TraceFinder for a minimum peak width of 0.21, maximum peak width of 0.84, and RT window set at 35 s, with retention time alignment and gap filling selected for exhaustive searching. Peak detection was performed by using an instrument-automated isotope cluster integration system (ICIS) algorithm. The mass tolerance for screening was 10 ppm in the full-scan mode. Thermo Scientific Freestyle was used for mass defects and isotopic pattern verification.

The in-built deconvolution feature of TraceFinder resulted in an extracted ion chromatogram (XIC), the illustration of which is shown in Fig. 2 for a magazine sample.

In suspect screening, XICs are important for removing background noise and baseline correction; in addition, it can assist in correcting repeating matrix effects. Deconvolution and background correction are also important when attempting to identify the PFAS present at trace levels (Liu et al., 2019). The Orbitrap MS^1 scan produced a forest of peaks that could be attributed to different types of organic chemical compounds present in the paper samples. In this study, PFAS compounds were of interest, and all other chemical classes were disregarded. Because the database libraries used were MS^1 level, it was important to be able to remove all background signals and matrix interferences from the full scan prior to database searching. A process of elimination or peak filtering was then employed to report the detected PFAS at as high a confidence level as possible. The advantage of advanced high-resolution accurate mass analysis is that the software can generate a monoisotopic mass, chemical formula, and isotopic mass pattern based on the acquired signal. The software further evaluates the observed isotopic pattern against the theoretically expected isotopic pattern based on the monoisotopic mass. The isotopic pattern observed for the tentatively identified 1,1,2,2-tetrafluorononane-3,5-dione is shown in Fig. 3, where all four possible isotopic fragments were observed for the [M − H] adduct as a molecular mass (M) of 227.0701 *m/z* at 5.93 min. Isotopic pattern matching is an important feature-filtering tool used to further increase the confidence of the identified compounds.



* S/N – signal-to-noise **RT – retention time

Fig. 1. Suspect screening protocol.

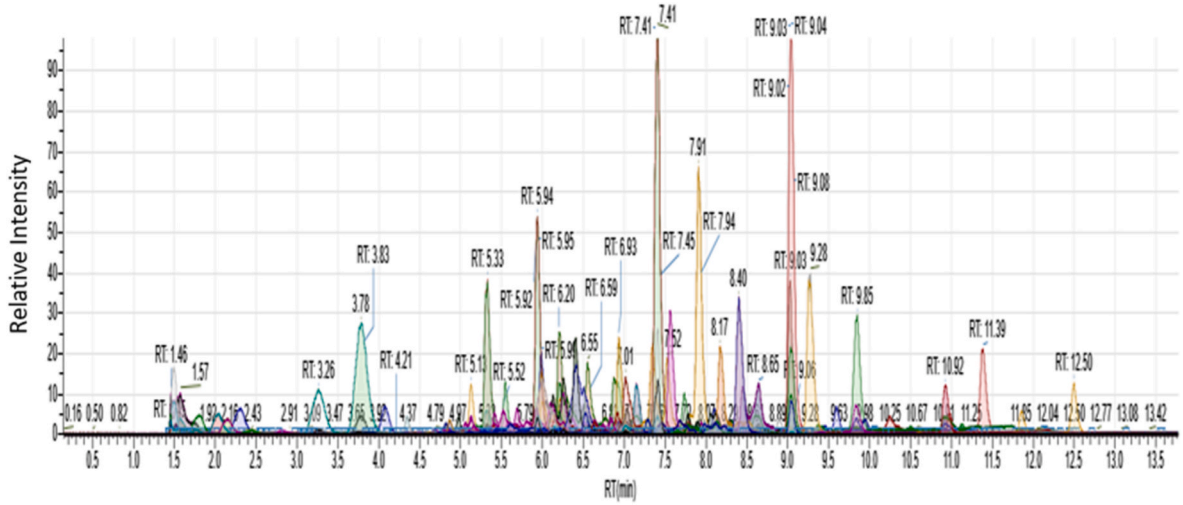


Fig. 2. XIC for magazine sample.

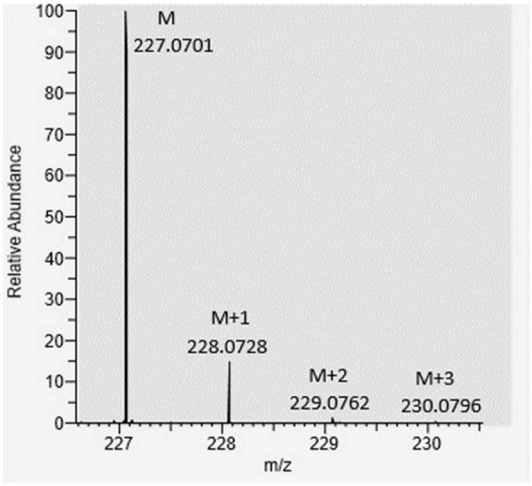
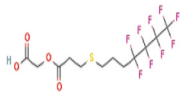
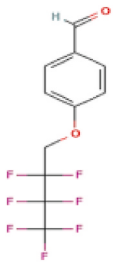
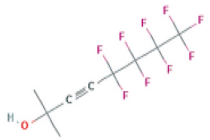


Fig. 3. Isotopic pattern for [M − H] 227.0701 *m/z*

3.2. Tentatively identified PFAS

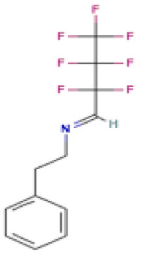
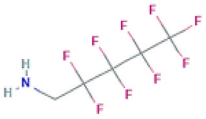
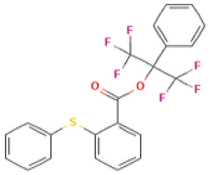
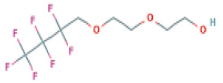
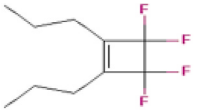
The suspected PFAS identified in this study are shown in Tables 1 and 2 for ASE with SPE and UAE-extracted samples, respectively. It is important to add that the ASE sample pre-treatment has already been shown to identify and quantify perfluorocarboxylic acid, perfluorosulphonic acids, and fluorotelomers in a targeted PFAS study (Anonymous, 2024). The reported compounds in this present study all had isotopic pattern scores of ≥80%, with the number of isotopes matched being ≥ n-1. Suspect screening was conducted on the premise of [M − H] adduct prominence. The compounds presented in Tables 1 and 2 were those obtained through the suspect screening workflow in Fig. 1 and were tentatively considered identification confidence level 3 according to (Charbonnet et al., 2022). The majority of the suspected compounds were found to have mass tolerances of less than 5 ppm, showing overall high accuracy and increased probability of positive identification. Five of the tentatively identified compounds were found to have a mass tolerance of less than 1 ppm, namely (1,1,1,3,3,3-hexafluoro-2-phenylpropan-2-yl) 2-phenylsulfanylbenzoate, 1-[4-(1-methylpropyl)phenoxy]-3-(2,2,3,3-tetrafluoropropoxy)- 2-propanol, 1-(2,2,3,3-tetrafluoropropyl)-1H-1,2,4-triazol-3-amine, N'-(benzenesulfonyl)-2,2,3,3,3-pentafluoro propanimidohydrazide and 1,1,1,2,2,3,3,4,4,5,5,6,6-tridecafluoro-8,8-dimethoxyoctane. MS^2 adds an additional layer of identification confidence. MS^2 fragments were acquired by DDA, in which abundant ions automatically initiated MS^2 fragmentation in the higher-energy collision-induced dissociation cell (HCD) with the instrument switching between full scan and MS^2 in a single run (Martinez-Bueno et al., 2019). Product ions were automatically assigned to the relevant precursor ions (Bugsel et al., 2023). The collision energy was stepped for ASE with SPE- and UAE-derived extracts at 15 and 30 eV. This indicated that the HCD energy switched between the two collision energies for each ion undergoing MS^2 fragmentation. The three most prominent MS^2 fragments are listed in Tables 1 and 2, respectively. The collision energy was not optimised for individual compounds; therefore, there was a strong possibility of insufficient collision energy. To illustrate, 4-(2,2,3,3,4,4,4-heptafluorobutoxy) benzaldehyde with an MS^1 precursor ion at 303.0269 *m/z* fragmented to *m/z* 80.9976, 222.7641, and 302.6823 (Table 1). The presence of 302.6823 *m/z* suggested insufficient fragmentation of the molecular ion. Although the use of DDA allowed for an automated link between the product ions and their associated precursor ions, the intensity threshold for fragmentation indicated that not all compounds triggered MS^2 fragmentation. This was also seen in Table 2, where ten identified PFAS MS^1 signals did not trigger MS^2 fragmentation. The lack of clean-up in the UAE-prepared samples meant that the sample matrix consisted of various classes of compounds that underwent full-scan acquisitions. The different ions present in each duty cycle could be present at higher intensities than the PFAS compounds, and would therefore be the preferred fragmentation candidates (Dickman and Aga, 2022). According to Furey et al. (2013), the analyte of interest in matrix components competes for the available charge, leading to either ion suppression or ion enhancement of the PFAS compounds (Furey et al., 2013). The specificity and selectivity of WAX SPE reduced the complexity of the samples and improved the intensities of MS^2 fragmentation, where all tentatively identified PFAS triggered fragmentation. For the MS^2 fragments, a confirmatory ion was identified using FreeStyle MS^2. The MS/MS Fragment generator in MStools was then used to identify the possible chemical composition of the fragments acquired, followed by a mass tolerance evaluation in order to further strengthen the confidence level of the tentative identification and to confirm that the compounds were of PFAS origin. The selected MS^2 ion and aligned retention time were then used to evaluate the presence of PFAS in the paper samples analysed. The majority of mass tolerances on MS^2 were less than 15 ppm for a majority of the compounds; however, a number of compounds had mass tolerances close to 30 ppm. In contrast, all MS^1 mass tolerances were less than 10 ppm. This indicated that analytical standards analysed under the same analytical conditions were required to truly optimize and confirm the ionization and fragmentation of the different PFAS compounds. Thermo FreeStyle was used to assess mass defect ranges as a possible data

Table 1
PFAS identified by ASE with SPE.

Chemical name	Chemical Formula	Chemical Structure*	RT	Monoisotopic Mass (amu)	$[M-H]^-$ Theoretical Mass m/z	$[M-H]^-$ Observed Mass (m/z)	MS^1 Mass tolerance (ppm)	Mass defect range (amu)	Confirmatory MS^2 fragments	Theoretical<Mass m/z	MS^2 Mass tolerance (ppm)
4:2 fluorotelomer thia propanoyl oxy propanoic acid	$C_{12}H_{13}F_9O_4S$		1.48	424.0391	423.0312	423.0333	4.96	−0.018 to 0.082	99.9945 $[C_2F_4]^-$	99.9936	9.00
5H-Perfluoropentanal	$C_5H_2F_8O$		1.49	229.9978	228.9899	228.9887	5.24	0.941 to 1.041	80.9956 $[C_2F_3]^-$	80.9952	4.94
2,2,3,3,4,4,5,5-Octafluoropentan-1-amine	$C_5H_5F_8N$		1.49	231.0294	230.0215	230.0218	1.30	−0.028 to 0.072	78.0177 $[C_2H_2F_2N]^-$	78.0155	28.20
4-(2,2,3,3,4,4,4-Heptafluorobutoxy) benzaldehyde	$C_{11}H_7F_7O_2$		1.52	304.0334	303.0255	303.0269	4.62	−0.024 to 0.076	80.9976$[C_2F_3]^-$	80.9952	29.63
5,5,6,6,7,7,8,8,8-Nonafluoro-2-methyloct-3-yn-2-ol	$C_9H_7F_9O$		1.52	302.0353	301.0274	301.0289	4.98	−0.022 to 0.078	68.9971 $[CF_3]^-$	68.9952	27.54
Difluoro(1,1,2,2-tetrafluoroethoxy) acetyl fluoride	$C_4HF_7O_2$		2.72	213.9865	212.9786	212.979	1.88	0.929 to 1.029	168.9884 $[C_3F_7]^-$	168.9888	2.37
1H-Heptafluoropropane	C_3HF_7		2.75	169.9966	168.9894	168.9887	3.96	0.939 to 1.039	68.9940 $[CF_3]^-$	68.9952	17.39

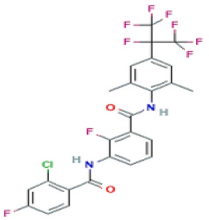
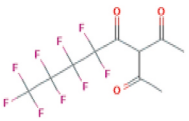
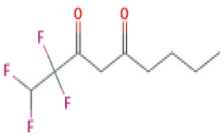
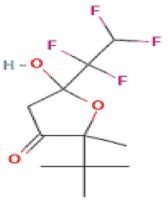
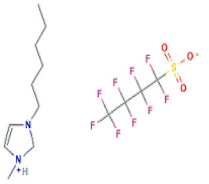
(*continued on next page*)

Table 1 (*continued*)

Chemical name	Chemical Formula	Chemical Structure*	RT	Monoisotopic Mass (amu)	$[M-H]^-$ Theoretical Mass *m/z*	$[M-H]^-$ Observed Mass (*m/z*)	MS^1 Mass tolerance (ppm)	Mass defect range (amu)	Confirmatory MS^2 fragments	Theoretical<Mass *m/z*	MS^2 Mass tolerance (ppm)
(1E)-2,2,3,3,4,4,4-Heptafluoro-N-(2-phenylethyl)butan-1-imine	$C_{12}H_{10}F_7N$		2.85	301.0701	300.0622	300.0639	5.67	0.013 to 0.113	115.0054 $[C_2HF_4N]$	115.0045	7.8
1H,1H-Perfluoropentylamine	$C_5H_4F_9N$		3.95	249.0200	248.0121	248.0115	2.42	−0.037 to 0.063	79.021 $[C_2H_3F_2N]^-$	79.0234	29.11
(1,1,1,3,3,3-hexafluoro-2-phenylpropan-2-yl) 2-phenylsulfanylbenzoate	$C_{22}H_{14}F_6O_2S$		3.88	456.0619	455.0540	455.0537	0.66	0.005 to 0.105	80.9955< $[C_2F_3]^-$	80.9952	3.70
1-(ethoxymethyl)-3-(2,2,3,3,4,4,5,5,6,6,7,7,8,8,8-pentadecafluorooctyl)urea	$C_{12}H_{11}F_{15}N_2O_2$		4.05	500.0581	499.0502	499.0526	4.81	0.001 to 0.101	106.0051 $[C_4HF_3]^-$	106.0030	19.81
2-[2-(2,2,3,3,4,4,4-Heptafluorobutoxy)ethoxy]ethan-1-ol	$C_8H_{11}F_7O_3$		4.31	288.0596	287.0517	287.0541	8.36	0.002 to 0.102	121.0108 $[C_4H_3F_2O_2]^-$	121.0101	5.78
3,3,4,4-tetrafluoro-1,2-dipropylcyclobutene	$C_{10}H_{14}F_4$		4.32	210.1032	209.0953	209.0947	2.68	0.046 to 0.146	118.0041 $[C_5HF_3]^-$	118.0030	9.32

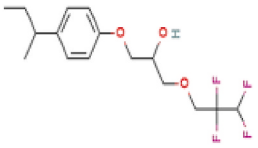
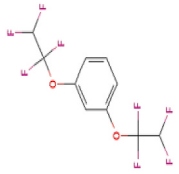
(*continued on next page*)

Table 1 (*continued*)

Chemical name	Chemical Formula	Chemical Structure*	RT	Monoisotopic Mass (amu)	$[M-H]^-$ Theoretical Mass m/z	$[M-H]^-$ Observed Mass (m/z)	MS^1 Mass tolerance (ppm)	Mass defect range (amu)	Confirmatory MS^2 fragments	Theoretical<Mass m/z	MS^2 Mass tolerance (ppm)
3-(2-Chloro-4-fluorobenzamido)-2-fluoro-N-[4-(1,1,1,2,3,3,3-heptafluoropropan-2-yl)-2,6-dimethylphenyl]benzamide	$C_{25}H_{16}ClF_9N_2O_2$		5.32	582.0756	581.0677	581.0671	1.03	0.018 to 0.118	198.0588 $[C_{10}H_7F_3N]^-$	198.0531	28.78
3-Acetyl-5,5,6,6,7,7,8,8,8-nonafluorooctane-2,4-dione	$C_{10}H_7F_9O_3$		5.37	346.0251	345.0172	345.0164	2.32	0.032 to 0068	80.9956 $[C_2F_3]^-$	80.9952	4.94
1,1,2,2-Tetrafluorononane-3,5-dione	$C_9H_{12}F_4O_2$		5.93	228.0773	227.0694	227.0701	2.95	0.02 to 0.12	80.9956 $[C_2F_3]^-$	80.9952	4.94
2-Tert-butyl-5-hydroxy-2-methyl-5-(1,1,2,2-tetrafluoroethyl)oxolan-3-one	$C_{11}H_{16}F_4O_3$		6.12	272.1036	271.0957	271.0978	7.89	0.046 to 0.146	80.9955 $[C_2F_3]^-$	80.9952	3.70
15,15,16,16,16-Pentafluorohexadecane-1-thiol	$C_{16}H_{29}F_5S$		6.53	348.1910	347.1831	347.1863	9.22	0.134 to 0.243	197.1361 $[C_{12}H_{21}S]^-$	197.1364	1.52
3-Hexyl-1-methyl-1H-Imidazolium perfluorobutane sulfonate	$C_{14}H_{21}F_9N_2O_3S$		6.82	468.1129	467.1050	467.1032	3.85	0.056 to 0.156	79.9556 $[SO_3]^-$	79.9568	15.01

(*continued on next page*)

Table 1 (*continued*)

Chemical name	Chemical Formula	Chemical Structure*	RT	Monoisotopic Mass (amu)	[M – H]⁻ Theoretical Mass *m/z*	[M – H]⁻ Observed Mass (*m/z*)	MS¹ Mass tolerance (ppm)	Mass defect range (amu)	Confirmatory MS² fragments	Theoretical<Mass *m/z*	MS² Mass tolerance (ppm)
1-[4-(1-methylpropyl)phenoxy]-3-(2,2,3,3-tetrafluoropropoxy)- 2-propanol	$C_{16}H_{22}F_4O_3$		8.38	338.1505	337.1426	337.1429	0.89	0.093 to 0.193	94.0249 $[C_3H_4F_2O]$	94.0230	20.21
1,3-Bis(1,1,2,2-tetrafluoroethoxy) benzene	$C_{10}H_6F_8O_2$		9.09	310.0240	309.0161	309.0175	4.53	−0.033 to 0.067	96.9889 $[C_2F_3O]^-$	96.9901	12.37

*Chemical structures are representative and do not show any branching.

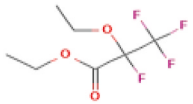
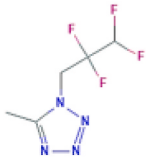
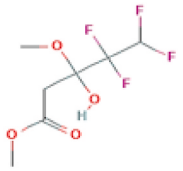
filtering step (Bugsel et al., 2023) using a relative mass defect filter of 50 mmu for a charge of −1 and hydrogen as the species. The premise of using mass defect filtering is the prominence of carbon and fluorine in typical PFAS compounds leading to an expected mass defect range of –0.25 Da from the negative fluorine contribution and +0.1 Da from the positive carbon contribution. The mass defect filter was outside the expected range for several compounds. This was attributed to the relatively short $–CF_2$ chains and the different heteroatoms present in the identified compounds, where carbon and hydrogen were associated with positive mass defects and the remaining chlorine, fluorine, iodine, nitrogen, and sulfur were associated with negative mass defects (Liu et al., 2022; Sleno, 2012). These results indicate that filtering compounds by mass defects could potentially result in overlooking the PFAS compounds. In this study, it was therefore employed for the purpose of verification and not as a data eliminating feature, as in non-target screening (Dickman and Aga, 2022; Koelmel et al., 2020; Bugsel and Zwiener, 2020; Liu et al., 2019, 2022).

3.3. Influence of selectivity on chemical characteristics of identified PFAS

In this study, various classes of PFAS were identified in the different paper samples. These PFAS compounds include perfluoroalkyl amines (2,2,3,3,4,4,5,5-octafluoropentan-1-amine and 1H,1H-perfluoropentylamine), polyfluoroalkyl diketones (1,1,2,2-tetrafluorononane-3,5-dione and 3-Acetyl-5,5,6,6,7,7,8,8,8-nonafluorooctane-2,4-dione), esters ((1,1,1,3,3,3-hexafluoro-2-phenylpropan-2-yl) 2-phenylsulfanylbenzoate ethyl 2-ethoxy-2,3,3,3-tetrafluoropropanoate), and fluorotelomer betaines (N-ethyl-N,N-dimethyl-(3-(difluoromethyl)perfluoropropyl)methan-1-aminium N-propyl-N,N-dimethyl-(3-(difluoromethyl)perfluoropropyl)methan-1-aminium). PFAS containing other halogens, (3-(2-chloro-4-fluorobenzamido)-2-fluoro-N-[4-(1,1,1,2,3,3,3-heptafluoropropan-2-yl)-2,6dimethylphenyl] benzamide, 4,4,5,5,6,6,7,7,8,8,8-undecafluoro-2-iodooctan-1-ol) as well as silyl alcohols, 1,1,1-trifluoro-5-(triethoxysilyl)-2-(trifluoromethyl)-2-pentanol, were also identified. The different classes of PFAS detected were strongly influenced by the applied extraction technique. UAE was observed to extract more nitrogen-containing compounds than ASE with the SPE. This was attributed to the pH selectivity caused by the weak anionic exchange mechanism (Taniyasu et al., 2023) targeting acidic carboxylic and sulfonic acids at pH < 6. UAE extraction was considered a generally more neutral extraction with a mixture at pH ~7, which may have been more favourable for quaternary ammonium compounds (fluorotelomer betaines). Confirmation with certified reference material would be important in further understanding this observation, reiterating the need for a broader range of commercially available PFAS standards. In addition to the pH-controlled sample pre-treatment, the mobile phase pH and matrix had a strong influence on the ionization efficiency. In the ASE with SPE, the mobile phase consisted of a buffered water system of 0.1 % formic acid with 10 mM ammonium formate, which resulted in a pH of 3.5 with a buffering range of 2.7–5.7. UAE sample preparation included buffering of both the aqueous phase and organic modifier to provide a consistent ionic state of the components in the complex matrix where no SPE had been performed. Stronger intensities were seen in ASE prepared samples which triggered MS^2 fragmentation indicating better ionization; however, this may have been due to less matrix interference after SPE. UAE allowed for the detection of different functional groups which inferred that the selectivity of SPE excluded some functional groups which could be important for suspect screening.

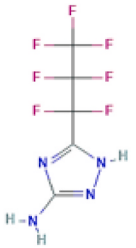
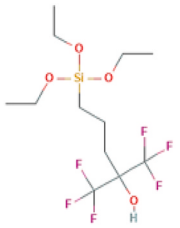
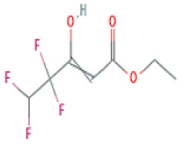
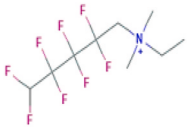
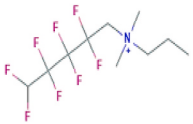
Concerns regarding PFAS have often been associated with the length of carbon chains present in PFAS. For PFCAs, carbon chains shorter than seven carbons and for PFSAs those less than six carbons, are considered short-chain PFAS and are believed to be less persistent than their longer chain counterparts (Grgas et al., 2023). The persistence of PFAS is associated with an extremely stable synthetic C–F bond (Berhanu et al., 2023). The PFAS identified from both extraction techniques were evaluated according to the length of the carbon chain and the length of the

Table 2
PFAS identified by UAE.

Chemical name	Chemical Formula	Chemical Structure*	RT	Monoiso-topic Mass (amu)	$[M-H]^-$ Theoreticalmass (m/z)	$[M-H]^-$ Observed Mass (m/z)	Mass tolerance (ppm)	Mass defect filtering range (Da)	MS^2 fragments acquired	TheoreticalMass m/z	MS^2 Mass tolerance (ppm)
Pentafluoropropane peroxoic acid	$C_3HF_5O_3H$		1.68	179.9846	178.9767	178.9773	−3.35	0.935 to 1.035	118.9958 $[C_2F_5]^-$	118.9920	31.93
4,4,5,5,6,6,7,7,8,8,8-Undecafluoro-2-iodooctan-1-ol	$C_8H_6F_{11}IO$		1.72	453.9288	452.9209	452.9215	−1.32	0.871 to 0.971	–		
ethyl 2-ethoxy-2,3,3,3-tetrafluoropropanoate	$C_7H_{10}F_4O_3$		1.75	218.0566	217.0487	217.0480	3.23	−0.001 to 0.099	68.9948 $[CF_3]^-$	68.9952	5.80
1-(2,2,3,3-Tetrafluoropropyl)-1H-1,2,4-triazol-3-amine	$C_5H_6F_4N_4$		2.62	198.0529	197.0450	197.0451	−0.51	0.004 to 0.096	–		
Methyl 4,4,5,5-tetrafluoro-3-hydroxy-3-methoxypentanoate	$C_7H_{10}F_4O_4$		4.08	234.0515	233.0436	233.0454	−7.72	−0.006 to 0.094	162.0134 $[C_6H_4F_2O_3]^-$	162.0129	3.09
1-(ethoxymethyl)-3-(2,2,3,3,4,4,5,5,6,6,7,7,8,8,8-pentadecafluorooctyl)urea	$C_{12}H_{11}F_{15}N_2O_2$		4.15	500.0581	499.0502	499.0527	−5,01	0.001 to 0.101	–		

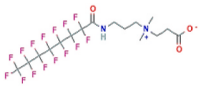
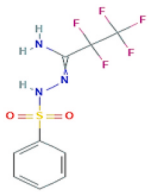
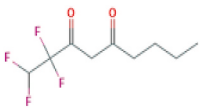
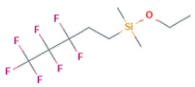
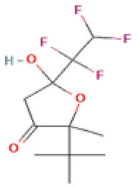
(*continued on next page*)

Table 2 (*continued*)

Chemical name	Chemical Formula	Chemical Structure*	RT	Monoiso-topic Mass (amu)	$[M-H]^-$ Theoreticalmass (m/z)	$[M-H]^-$ Observed Mass (m/z)	Mass tolerance (ppm)	Mass defect filtering range (Da)	MS^2 fragments acquired	TheoreticalMass m/z	MS^2 Mass tolerance (ppm)
3-(Heptafluoropropyl)-1H-1,2,4-triazol-5-amine	$C_5H_3F_7N_4$		4.16	252.0246	251.0167	251.0183	−6,41	−0.033 to 0.067	–		
N-Carboxymethyl-N,N-dimethyl-2-(perfluoropropyl)-2-fluoroethan-1-aminium	$C_9H_{12}F_8NO_2$		4.31	318.0740	317.0661	317.0665	−1,26	0.017 to 0.117	–		
1,1,1-trifluoro-5-(triethoxysilyl)-2-(trifluoromethyl)- 2-pentanol	$C_{12}H_{22}F_6O_4Si$		4.50	372.1192	371.1113	371.1138	−6,74	0.062 to 0.162	97.9995 $[C_2HF_3O]^-$	97.9979	16.33
Ethyl 4,4,5,5-tetrafluoro-3-hydroxypent-2-enoate	$C_7H_8F_4O_3$		5.03	216.0409	215.0330	215.0346	−7.44	−0.016 to 0.084	–		
N-Ethyl-N,N-dimethyl-(3-(difluoromethyl)perfluoropropyl) methan-1-aminium	$C_9H_{14}F_8N$		5.16	288.0998	287.0919	287.0925	−2.09	0.043 to 0.143	–		
N-Propyl-N,N-dimethyl-(3-(difluoromethyl)perfluoropropyl) methan-1-aminium	$C_{10}H_{16}F_8N$		5.16	302.1155	301.1076	301.1082	−1.99	0.058 to 0.158	99.9918 $[C_2F_4]^-$	99.9936	18.00

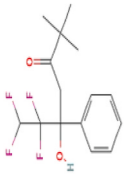
(*continued on next page*)

Table 2 (*continued*)

Chemical name	Chemical Formula	Chemical Structure*	RT	Monoiso-topic Mass (amu)	$[M-H]^-$ Theoreticalmass (m/z)	$[M-H]^-$ Observed Mass (m/z)	Mass tolerance (ppm)	Mass defect filtering range (Da)	MS^2 fragments acquired	TheoreticalMass m/z	MS^2 Mass tolerance (ppm)
(2-Carboxylatoethyl)dimethyl[3-(perfluorooctanamido)propyl] ammonium	$C_{16}H_{17}F_{15}N_2O_3$		5.28	570.0999	569.0920	569.0945	−4.39	0.043 to 0.143	–		
N'-(Benzenesulfonyl)-2,2,3,3,3-pentafluoropropanimidohydrazide	$C_9H_8F_5N_3O_2S$		5.32	317.0257	316.0178	316.0178	0.95	−0.032 to 0.068	111.9921 $[CF_4]^-$	111.9936	13.39
N-dimethylammoniocarboxypropyl perfluoroethane sulphonamide	$C_8H_{13}F_5N_2O_4S$		5.53	328.0516	327.0437	327.0444	−2.14	−0.006 to 0.094	158.9648 $[C_2F_3NO_2S]^-$	158.9602	28.94
1,1,1,2,2,3,3,4,4,5,5,6,6-Tridecafluoro-8,8-dimethoxyoctane	$C_{10}H_9F_{13}O_2$		5.75	408.0395	407.0316	407.0319	−0.74	−0.018 to 0.082	–		
1,1,1,2,2,3,3,4,4,5,5,6,6-Tridecafluorohexadecane	$C_{16}H_{21}F_{13}$		5.75	460.1436	459.1357	459.1340	3.70	0.086 to 0.186	–		
1,1,2,2-Tetrafluorononane-3,5-dione	$C_9H_{12}F_4O_2$		5.83	228.0773	227.0694	227.0710	−7.05	−0.001 to 0.099	–		
Ethoxydimethyl (3,3,4,4,5,5,5-heptafluoropentyl) silane	$C_9H_{15}F_7OSi$		5.84	300.0780	299.0701	299.0716	−5.02	0.02 to 0.12	255.0506 $[C_7H_{10}F_7Si]^-$	255.0440	25.88
2-Tert-butyl-5-hydroxy-2-methyl-5-(1,1,2,2-tetrafluoroethyl)oxolan-3-one	$C_{11}H_{16}F_4O_3$		5.92	272.1036	271.0957	271.0977	−7.53	0.021 to 0.121	99.9918 $[C_2F_4]^-$	99.9936	18.00

(*continued on next page*)

Table 2 (*continued*)

Chemical name	Chemical Formula	Chemical Structure*	RT	Monoisotopic Mass (amu)	$[M-H]^-$ Theoreticalmass (*m/z*)	$[M-H]^-$ Observed Mass (*m/z*)	Mass tolerance (ppm)	Mass defect filtering range (Da)	MS^2 fragments acquired	TheoreticalMass *m/z*	MS^2 Mass tolerance (ppm)
1,1,1,2-Tetrafluorononan-3-one	$C_9H_{14}F_4O$		6.03	214.0981	213.0902	213.0917	−7.04	0.046 to 0.146	197.0601 $[C_8H_9F_4O]^-$	197.0590	5.58
3,3,4,4,5,5,6,6,7,7-Decafluorooctyl 2-methylprop-2-enoate	$C_{12}H_{12}F_{10}O_2$		6.10	378.0677	377.0598	377.0604	−1.59	0.041 to 0.141	80.9940 $[C_2F_3]^-$	80.9952	14.82
6,6,7,7-Tetrafluoro-5-hydroxy-2,2-dimethyl-5-phenylheptan-3-one	$C_{15}H_{18}F_4O_2$		6.37	306.1243	305.1185	305.1164	−6.88	0.01 to 0.11	111.9917 $[C_3F_4]^-$	111.9936	16.97

fluoroalkyl chain (Fig. 4). Significant differences were noted for 15,15,16,16,16-pentafluorohexadecane-1-thiol (C-chain of 16 carbons, CF-chain of 2), 1,1,1,2,2,3,3,4,4,5,5,6,6-tridecafluorohexadecane (C-chain 16 and CF-chain 6) and 3-hexyl-1-methyl-1H-imidazolium perfluorobutane sulfonate (C-chain 10 and CF-chain of 4). Although these compounds would be considered short-chain PFAS (Ateia et al., 2019), their associated aliphatic chains were greater than the nine carbons chain long which suggested that further understanding of their overall stability in the paper recycling chain is required. This is especially important when considering the other functional groups present such as esters, ethers, amines, exposure pathways and related toxicity (McKee et al., 2018; Grgas et al., 2023).

It must be highlighted that the reported PFAS in this study were those that met the confidence interval threshold discussed in section 3.1. Although the advantage of having higher confidence intervals increases the probability of correct identification, the limitation is that it may exclude chemical compounds that may not act in the theoretically expected manner, further emphasizing the need for PFAS reference material. Illustratively, if the threshold for accurate mass were set to accurate mass threshold <15 ppm instead of the set <10 ppm and the isotopic mass fragment increased to > n-2 instead of the set > n-1, 3,3,4,4,5,5,6,6,7,7,8,8,8-tridecafluorooctyl isobutyrate ($C_{12}H_{11}F_{13}O2$) detected in the corrugated box collected at a recycling facility by UAE would then be included in this tentative identification study. It can thus be said that the balance between explorative untargeted analysis and the corroborative features selected for confident tentative identification is important in expanding PFAS knowledge on occurrences. More importantly, it indicates that the absence of the required evidence for identification may not, at this stage, mean that the PFAS in question is not detected; it merely means that it cannot be confidently reported on.

3.4. Distribution of identified PFAS in samples

The PFAS detected in the paper samples were compared to evaluate the distribution of PFAS from the combined pre-treatment methods (Tables 3 and 4). 2-*tert*-butyl-5-hydroxy-2-methyl-5-(1,1,2,2-tetrafluoroethyl)oxolan-3-one was detected in the highest number of samples across various sites. This suggests a possible prevalent use in paper manufacturing, which has not been previously reported. In contrast, 3-(2-chloro-4-fluorobenzamido)-2-fluoro-N-[4-(1,1,1,2,3,3,3-heptafluoropropan-2-yl)-,6-dimethylphenyl]benzamide was detected in household waste, recycling, and waste picker samples suggesting prevalence in or exposure related to post-consumer usage, waste collection, and recovery. Only 3 common PFAS were identified in both ASE and UAE prepared samples. These were 2-*tert*-butyl-5-hydroxy-2-methyl-5-(1,1,2,2-tetra fluoroethyl)oxolan-3-one, 1,1,2,2-tetrafluorononane-3,5-dione and 1-(ethoxymethyl)-3-(2,2,3,3,4,4,5,5,6,6,7,7,8,8,8-pentadecafluoro octyl) urea. This suggested that method specificity and selectivity highly influenced by the method of extraction, implying the need for applying both methods when conducting suspect screening of PFAS. This would not only be relevant to analytical identification, but would be influential in how certain PFAS are removed in recycled material and process waters. The corrugated electronics box sourced from retail had the most tentatively identified PFAS (10 of the 41 PFAS) detected when both sample preparation results were considered in conjunction.

The sources of most PFAS are difficult to establish as the research field is emerging, and information from chemical manufacturers in the form of disclosures and patents is limited (Glüge et al., 2020). Different functional groups have been studied to determine their occurrence. Fluorinated aldehydes are oxidation products of alcohols and can form from the reduction of carboxylic acid; microbial degradation of fluorotelomers is known to generate aldehydes and PFCAs under aerobic conditions (Berhanu et al., 2023). Fluoro ether substances, on the other hand, are among the current alternatives to long-chain perfluoroalkyl acids (Munoz et al., 2019) whereas perfluoroalkyl butoxy ethoxy ethanols are used as fluorinated surfactants (Paborn and Caport, 2002).

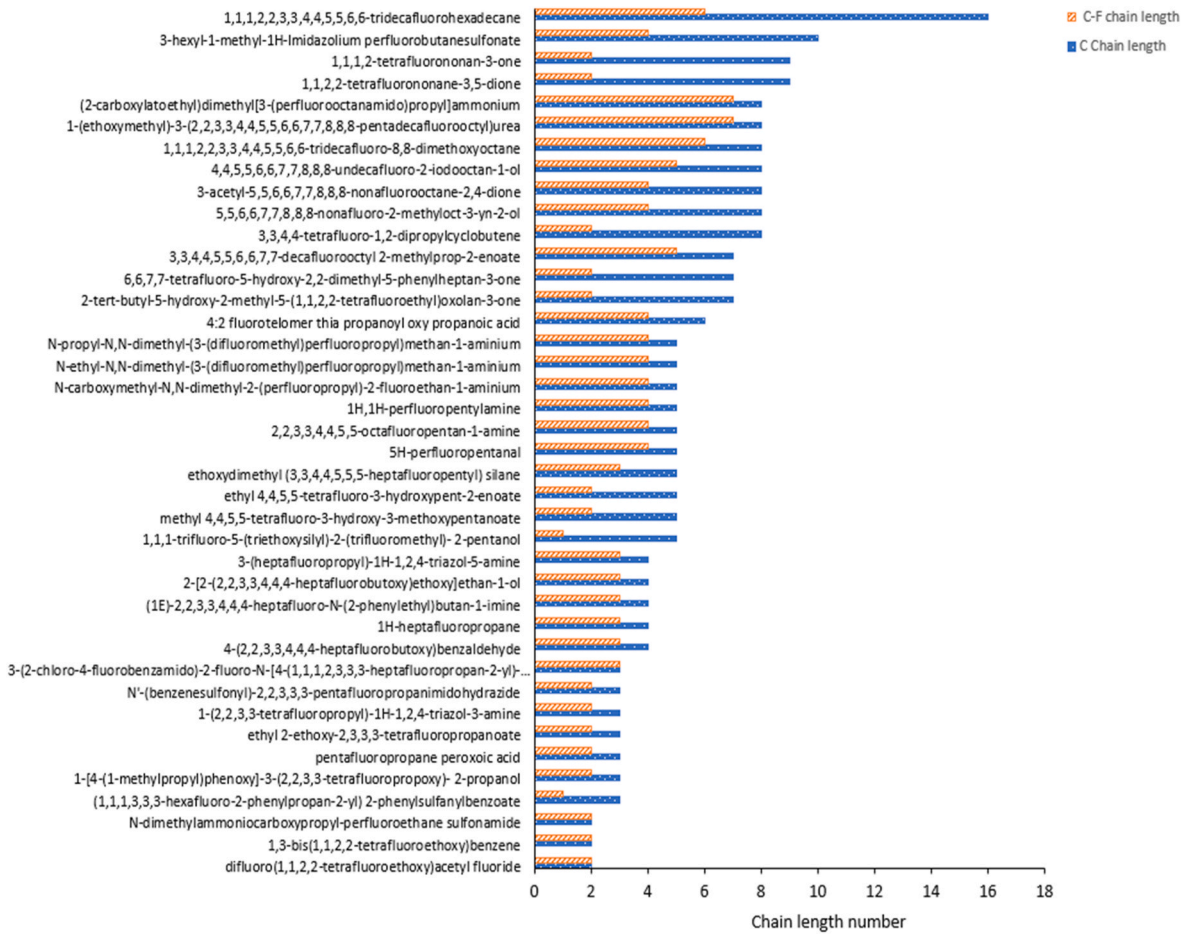


Fig. 4. Carbon chain lengths of identified PFAS.

Perfluoroalkylethyl iodides can be readily converted to their corresponding alcohols, thiols, and sulfonyl chlorides, which are used as intermediates for fluorinated surfactants (Paborn and Caport, 2002). Interestingly, UAE extraction led to the detection of fluorotelomer betaines, which have been previously detected in samples of different origins, including aqueous film-forming foams and fluoro surfactants, as well as soil and groundwater (Li et al., 2019; Liu et al., 2022; Munoz, 2016). This class of PFAS has also been detected in biosolids, composts, and organic wastes (Munoz et al., 2022). The exposure of paper to similar organic wastes could be a possible reason for its detection in this study. It is difficult to apportion PFAS prevalence to a specific source, as PFAS undergo diverse transformations, transport, partitioning, and degradation processes (Grgas et al., 2023). Further studies are required to fully explore various exposure pathways, mechanisms, and transformations that may occur in the paper recycling chain.

The average integrated peak areas were used as indicators of the general abundance. For PFAS, it must be noted that the instrument response is dependent on matrix effects and ionization efficiency (Tang et al., 2023). Another challenge associated with PFAS quantitation is poor recovery (Tang et al., 2023). The influence of the type of pre-treatment used is evident in Figs. 5 and 6 for the PFAS identified by ASE with SPE and UAE, respectively. The commonly detected 2-*tert*-butyl-5-hydroxy-2-methyl-5-(1,1,2,2-tetra fluoroethyl)oxolan-3-one and 1,1,2,2-tetrafluorononane-3,5-dione were detected more frequently in pre-treatment by UAE than by ASE with SPE whilst 1-(ethoxymethyl)-3-(2,2,3,3,4,4,5,5,6,6,7,7,8,8,8-pentadecafluorooctyl) urea was detected more in ASE with SPE than UAE. This was influenced by the slight differences in solvents used in the pre-treatment techniques as well as the selectivity introduced by SPE. The possible prevalence of certain PFAS in the paper recycling chain was inferred by the common detection of 3-acetyl-5,5,6,6,7,7,8,8,8-nonafluorooctane-2, 4-dione by ASE with SPE (in Fig. 5) as well as 2-*tert*-butyl-5-hydroxy-2-methyl-5-(1,1,2,2-tetra fluoroethyl)oxolan-3-one and 1,1,2,2-tetrafluorononane-3,5-dione detected by UAE (Fig. 6) across the collection sites. Their abundance in this study implied the possible prevalence of short-chain polyfluoroalkyl ketones and diketones in the paper recycling chain. On the other hand, certain PFAS such as perfluoropentanal, detected in an infant bath packaging household sample from ASE with SPE, were unique in their identification. When comparing the number of different PFAS identified for both sample pre-treatment techniques, more types of PFAS were identified in an electronics box and toy box, both collected at retail. This suggested that sources of PFAS could also be related to the goods packed in paper-based packaging; in addition to activities related to the use of chemical additives, as well as handling, transport and distribution exposure opportunities. Overall, the tentatively identified PFAS indicated that there were several common previously unreported PFAS in the paper recycling chain as well as those that were unique to different collection sites and samples. Further research and the availability of analytical standards are needed to accurately quantify these PFAS and understand their occurrence in paper-based material and possibly environmental media.

4. Conclusion

This study developed a systematic approach to suspect screening linked to confidence level. The peak filtering and thresholds employed increased the probability of correct identification while reducing false-positive reporting. This study highlighted the importance of extraction

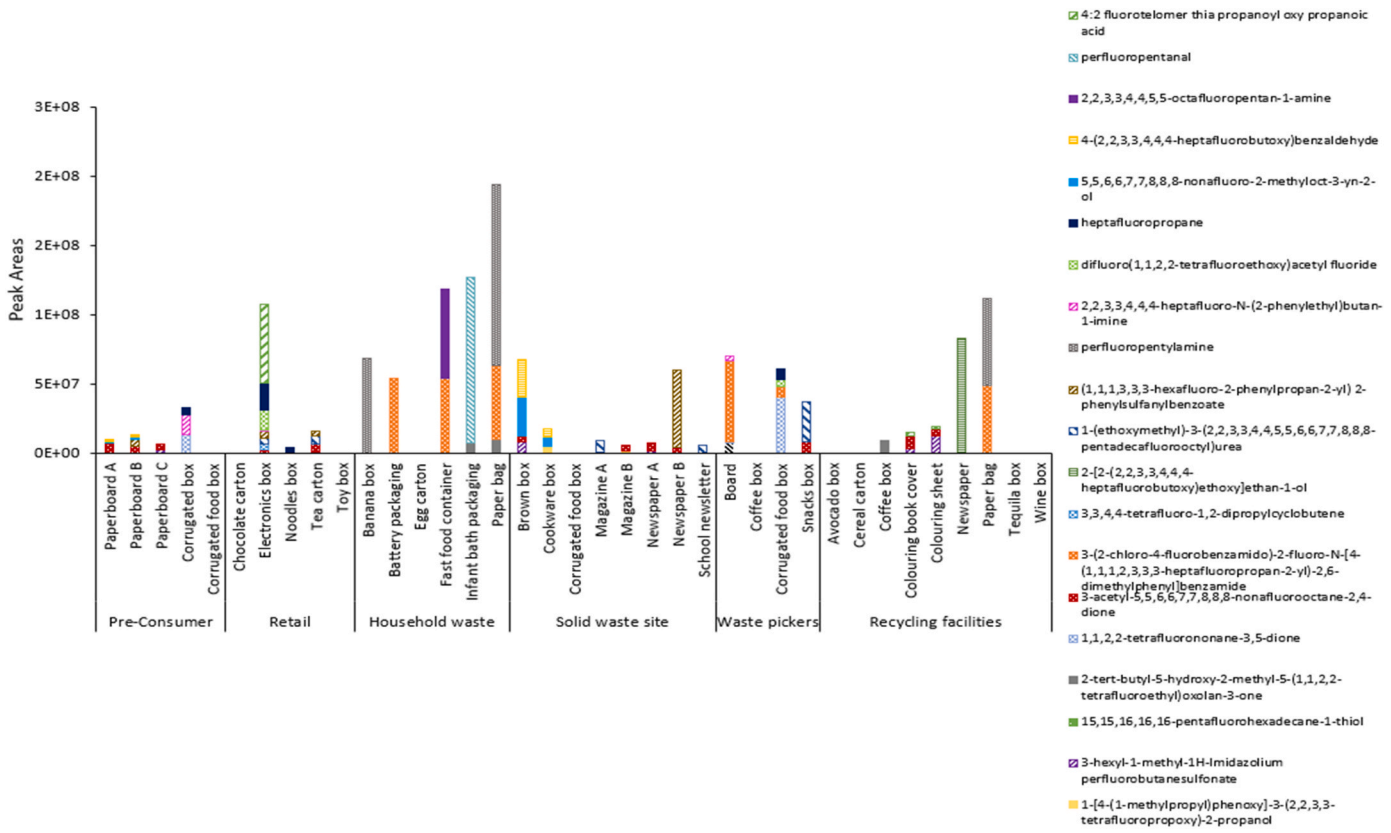


Fig. 5. Peak areas of identified PFAS from ASE with SPE sample pre-treatment.

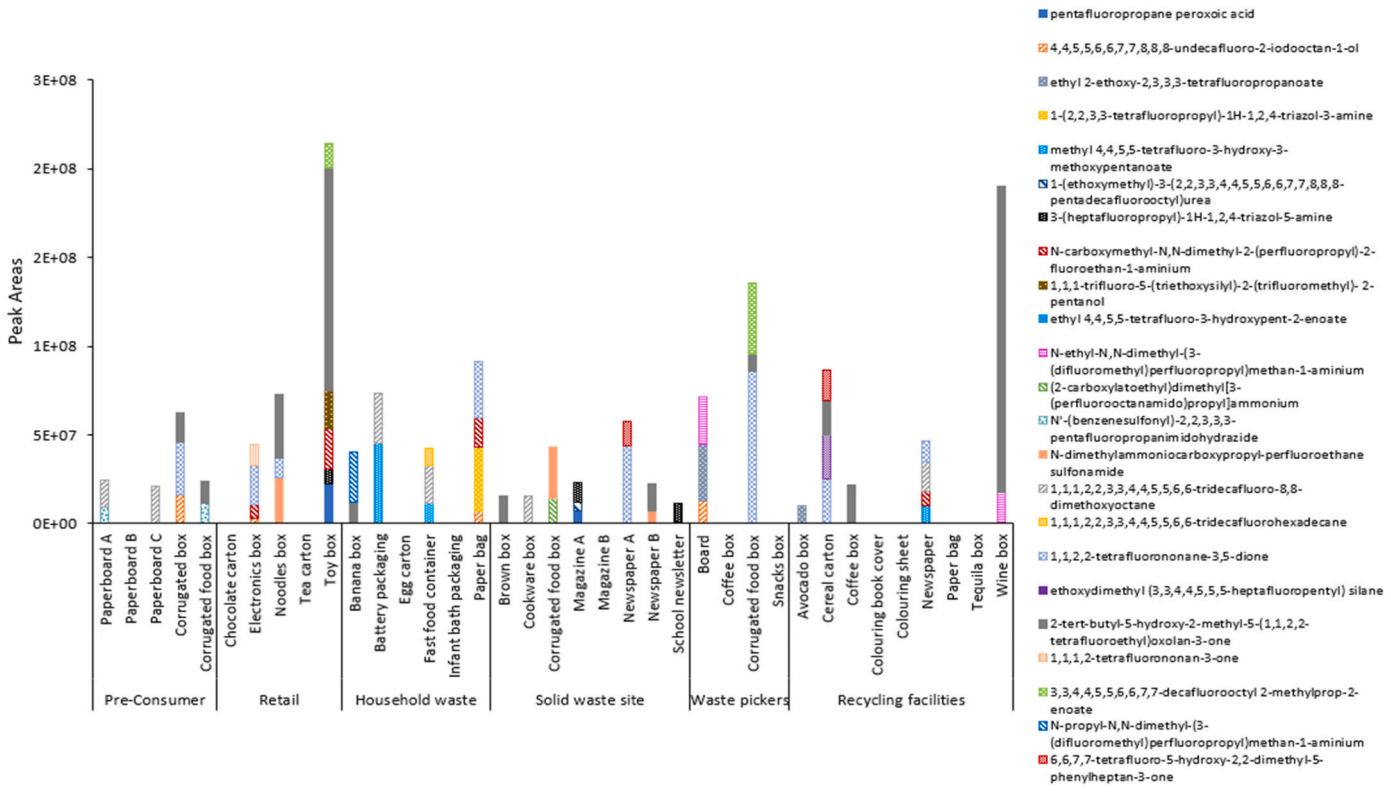


Fig. 6. Average peak areas of identified PFAS from UAE sample pre-treatment.

techniques, acquisition mechanisms, and data processing in PFAS screening. ASE with SPE sample preparation identified 21 suspected PFAS with MS^2 fragmentation. UAE was able to tentatively identify 23 PFAS; however, not all suspected PFAS were able to trigger MS^2 fragmentation, as a result of DDA acquisition. Fluoroalkyl amines, diketones, betaines, and silyl alcohols are among the different functional groups identified. The study highlighted that further exploration is required to understand the complexities of PFAS, their risks, and their applications.

CRediT authorship contribution statement

Nondumiso N. Mofokeng: Writing – original draft, Project administration, Methodology, Formal analysis, Data curation, Conceptualization. **Lawrence M. Madikizela:** Writing – review & editing, Validation, Supervision, Data curation. **Ineke Tiggelman:** Writing – review & editing, Validation, Project administration, Data curation. **Edmond Sanganyado:** Writing – review & editing, Validation, Conceptualization. **Luke Chimuka:** Writing – review & editing, Validation, Supervision, Project administration.

Declaration of competing interest

The authors declare the following financial interests/personal relationships which may be considered as potential competing interests: Nondumiso Mofokeng reports funding was provided by Mpact Operations Pty (Ltd). All other authors declare that they have no known competing financial interests or personal relationships that could have appeared to influence the work reported in this paper.

Data availability

Data will be made available on request.

Acknowledgments

Mpact Operations Pty (Ltd) Innovation, Research and Development division is acknowledged for financial support. Anatech Instruments Pty (Ltd) is thanked for the Thermo Scientific Vanquish UHPLC+ Q Exactive Focus Orbitrap.

Appendix A. Supplementary data

Supplementary data to this article can be found online at https://doi.org/10.1016/j.chemosphere.2024.142904.

References

Al Amin, M., Sobhani, Z., Liu, Y., Dharmaraja, R., Chadalavada, S., Naidu, R., et al., 2020. Recent advances in the analysis of per- and polyfluoroalkyl substances (PFAS)—a review. Environ. Technol. Innovat. 19, 100879 https://doi.org/10.1016/j.eti.2020.100879.

Anonymous, 2024.

Ateia, M., Maroli, A., Tharayil, N., Karanfil, T., 2019. The overlooked short- and ultrashort-chain poly- and perfluorinated substances: a review. Chemosphere 220, 866–882. https://doi.org/10.1016/j.chemosphere.2018.12.186.

Baduel, C., Mueller, J.F., Rotander, A., Corfield, J., Gomez-Ramos, M.J., 2017. Discovery of novel per- and polyfluoroalkyl substances (PFASs) at a fire fighting training ground and preliminary investigation of their fate and mobility. Chemosphere 185, 1030–1038. https://doi.org/10.1016/j.chemosphere.2017.06.096.

Berhanu, A., Mutanda, I., Taolin, J., Qaria, M.A., Yang, B., Zhu, D., 2023. A review of microbial degradation of per- and polyfluoroalkyl substances (PFAS): biotransformation routes and enzymes. Sci. Total Environ. 859, 160010 https://doi.org/10.1016/j.scitotenv.2022.160010.

Boisacq, P., De Keuster, M., Prinsen, E., Jeong, Y., Bervoets, L., Eens, M., et al., 2023. Assessment of poly- and perfluoroalkyl substances (PFAS) in commercially available drinking straws using targeted and suspect screening approaches. Food Addit. Contam. 40, 1230–1241. https://doi.org/10.1080/19440049.2023.2240908.

Bugsel, B., Zwiener, C., 2020. LC-MS screening of poly- and perfluoroalkyl substances in contaminated soil by Kendrick mass analysis. Anal. Bioanal. Chem. 412, 4797–4805. https://doi.org/10.1007/s00216-019-02358-0.

Bugsel, B., Zweigle, J., Zwiener, C., 2023. Nontarget screening strategies for PFAS prioritization and identification by high resolution mass spectrometry: a review. Environ.Anal.Chem 40, e00216. https://doi.org/10.1016/j.teac.2023.e00216.

Charbonnet, J.A., McDonough, C.A., Xiao, F., Schwichtenberg, T., Cao, D., Kaserzon, S., et al., 2022. Communicating confidence of per- and polyfluoroalkyl substance identification via high-resolution mass spectrometry. Environ. Sci. Technol. Lett. 9, 473–481. https://doi.org/10.1021/acs.estlett.2c00206.

Dickman, R.A., Aga, D.S., 2022. Efficient workflow for suspect screening analysis to characterize novel and legacy per- and polyfluoroalkyl substances (PFAS) in biosolids. Anal. Bioanal. Chem. 414, 4497–4507. https://doi.org/10.1007/s00216-022-04088-2.

EPA PFAS Chemicals list, 2022. CompTox chemicals dashboard. accessed from. https://comptox.epa.gov/dashboard/chemical-lists.

Furey, A., Moriarty, M., Bane, V., Kinsella, B., Lehane, M., 2013. Ion suppression; A critical review on causes, evaluation, prevention and applications. Talanta 115, 104–122. https://doi.org/10.1016/j.talanta.2013.03.048.

Getzinger, G.J., Higgins, C.P., Ferguson, P.L., 2021. Structure database and in silico spectral library for comprehensive suspect screening of per- and polyfluoroalkyl substances (PFASs) in environmental media by high-resolution mass spectrometry. Anal. Chem. 93, 2820–2827. https://doi.org/10.1021/acs.analchem.0c04109.

Glüge, J., Scheringer, M., Cousins, I.T., Dewitt, J.C., Goldenman, G., Herzke, D., et al., 2020. An overview of the uses of per- and polyfluoroalkyl substances (PFAS). Environ. Sci. J. Integr. Environ. Res.: Process. Impacts 22, 2345–2373. https://doi.org/10.1039/d0em00291g.

Grgas, D., Petrina, A., Štefanac, T., Bešlo, D., Landeka Dragičević, T., 2023. A review: per- and polyfluoroalkyl substances—biological degradation. Toxics 11, 446. https://doi.org/10.3390/toxics11050446.

Hajeb, P., Zhu, L., Bossi, R., Vorkamp, K., 2022. Sample preparation techniques for suspect and non-target screening of emerging contaminants. Chemosphere 287, 132306.

Houtz, E., Wang, M., Park, J., 2018. Identification and fate of aqueous film forming foam derived per- and polyfluoroalkyl substances in a wastewater treatment plant. Environ. Sci. Technol. 52 (22), 13212–13221. https://doi.org/10.1021/acs.est.8b04028.

Koelmel, J.P., Paige, M.K., Aristizabal-Henao, J.J., Robey, N.M., Nason, S.L., Stelben, P. J., et al., 2020. Toward comprehensive per- A nd polyfluoroalkyl substances annotation using FluoroMatch software and intelligent high-resolution tandem mass spectrometry acquisition. Anal. Chem. 92, 11186–11194. https://doi.org/10.1021/acs.analchem.0c01591.

Liu, L., Lu, M., Cheng, X., Yu, G., Huang, J., 2022. Suspect screening and nontargeted analysis of per- and polyfluoroalkyl substances in representative fluorocarbon surfactants, aqueous film-forming foams, and impacted water in China. Environ. Int. 167, 107398 https://doi.org/10.1016/j.envint.2022.107398.

Liu, Y., D'Agostino, L.A., Qu, G., Jiang, G., Martin, J.W., 2019. High-resolution mass spectrometry (HRMS) methods for nontarget discovery and characterization of poly- and per-fluoroalkyl substances (PFASs) in environmental and human samples. TrAC, Trends Anal. Chem. 121, 115420 https://doi.org/10.1016/j.trac.2019.02.021.

Manojkumar, Y., Pilli, S., Rao, P.V., Tyagi, R.D., 2023. Sources, occurrence and toxic effects of emerging per- and polyfluoroalkyl substances (PFAS). Neurotoxicol. Teratol. 97, 107174 https://doi.org/10.1016/j.ntt.2023.107174.

McKee, R.H., Tibaldi, R., Adenuga, M.D., Carrillo, J.-C., Margary, A., 2018. Assessment of the potential human health risks from exposure to complex substances in accordance with REACH requirements. "White spirit" as a case study. Regul. Toxicol. Pharmacol. 92, 439–457. https://doi.org/10.1016/j.yrtph.2017.10.015.

Munoz, G., Michaud, A.M., Liu, M., Duy, S.V., Resseguier, D.M.C., et al., 2022. Target and nontarget screening of PFAS in biosolids, composts, and other organic waste products for land application in France. Environ. Sci. Technol. 56, 6056–6068. https://doi.org/10.1021/acs.est.1c03697.

Paborn, M., Caport, J.M., 2002. Fluorinated surfactants: synthesis, properties, effluent treatment. J. Fluor. Chem. 114 (2), 149–156. https://doi.org/10.1016/S0022-1139(02)00038-6.

Place, B., 2021. Suspect List of Possible Per- and Polyfluoroalkyl Substances (PFAS). National Institute of Standards and Technology. https://doi.org/10.18434/mds2-2387. https://data.nist.gov/od/id/mds2-2387.

Sapozhnikova, Y., Taylor, R.B., Bedi, M., Ng, C., 2023. Assessing per- and polyfluoroalkyl substances in globally sourced food packaging. Chemosphere 337, 139381. https://doi.org/10.1016/j.chemosphere.2023.139381.

Shen, Y., Wang, L., Ding, Y., Liu, S., Li, Y., Zhou, Z., et al., 2023. Trends in the analysis and exploration of per- and polyfluoroalkyl substances (PFAS) in environmental matrices: a review. Crit. Rev. Anal. Chem. 6, 1–25. https://doi.org/10.1080/10408347.2023.2231535.

Sleno, L., 2012. The use of mass defect in modern mass spectrometry. J. Mass Spectrom. 47, 226–236. https://doi.org/10.1002/jms.2953.

Stroski, K.M., Sapozhnikova, Y., 2023. Analysis of per- and polyfluoroalkyl substances in plastic food storage bags by different analytical approaches. J.Chromatography. 4, 100106 https://doi.org/10.1016/j.jcoa.2023.100106.

Tang, C., Liang, Y., Wang, K., Liao, J., Zeng, Y., Luo, X., et al., 2023. Comprehensive characterization of per- and polyfluoroalkyl substances in wastewater by liquid chromatography-mass spectrometry and screening algorithms. Npj Clean Water 6, 6. https://doi.org/10.1038/s41545-023-00220-6.

Trier, X., Granby, K., Christensen, J.H., 2011. Tools to discover anionic and nonionic polyfluorinated alkyl surfactants by liquid chromatography electrospray ionisation mass spectrometry. J. Chromatogr. A 1218, 7094–7104. https://doi.org/10.1016/j.chroma.2011.07.057.

Wang, Y., Yu, N., Zhu, X., Guo, H., Jiang, J., Wang, X., et al., 2018. Suspect and nontarget screening of per- and polyfluoroalkyl substances in wastewater from a fluorochemical manufacturing park. Environ. Sci. Technol. 52, 11007–11016.

Wang, Z., Buser, A.M., Cousins, I.T., Demattio, S., Drost, W., Johansson, O., Ohno, K., Patlewicz, G., et al., 2021. New OECD definition for per- and polyfluoroalkyl substances. Environ. Sci. Technol. 55 (23), 15575–15578. https://doi.org/10.1021/acs.est.1c06896.

Wang, Y.Q., Hu, L.X., Liu, T., Zhao, J.H., Yang, Y.Y., Liu, Y.S., et al., 2022. Per- and polyfluoralkyl substances (PFAS) in drinking water system: target and non-target screening and removal assessment. Environ. Int. 163, 107219 https://doi.org/10.1016/j.envint.2022.107219.

Zweigle, J., Bugsel, B., Röhler, K., Haluska, A.A., Zwiener, C., 2023. PFAS-contaminated soil site in Germany: nontarget screening before and after direct TOP assay by kendrick mass defect and FindPFΔS. Environ. Sci. Technol. 57, 6647–6655. https://doi.org/10.1021/acs.est.2c07969.